Model-Based Compensation of Friction in Direct-Drive Robotic Arms

Milos R. Popovic and Andrew A. Goldenberg

Robotics and Automation Laboratory
Mechanical Engineering Department
University of Toronto
5,King's College Road,
Toronto,Ontario M5S 1A4
CANADA

Karun B. Shimoga

The Robotics Institute
Carnegie Mellon University
Pittsburgh, PA 15213
USA

Raymond C.Hui

Canadian Space Agency
P.O.Box 11490 Stn. H,
Ottawa, Ontario K2H 8S2
CANADA

Abstract: It is often assumed that the friction in direct-drive motors is negligible. However, experimental work has proved that friction significantly influences the performance of direct-drive motors. The Tustin's model has been used here for feedforward model-based compensation. It was found that the magnitude of the velocity and of the controller gains determine the required extent of the model-based compensation. This compensation method improved the performance of the direct-drive motors, particularly at the low velocity.
Keywords: Friction, modelling, compensation and direct-drive motors.

1. Introduction

The recent trend towards direct-drive robot manipulators in experimental research has largely been motivated by practical problems associated with the use of gear and pulley transmission systems. It was found that friction is a major problem in such actuators.

There are three approaches to compensate for friction, published in the literature. The first, and the simplest method involves the use of large gains in the manipulator feedback control. The second strategy is based on high frequency signals, also known as dither signals. Finally, model-based compensation is the most theoretically rigorous method, and is the main concern in this paper. In particular, the model-based compensation employs a model of friction force which describes friction variation over the operating velocity range of the manipulator joint under study. On-line estimated friction force can further be used for calculating the necessary compensation.

In this paper, we intend to present the results of our experiments with a two link direct-drive manipulator (Figure 1) aimed at determining the friction model and using it in feedforward compensation. The results confirm that the direct-drive manipulators are not immune to the friction effect, as very often assumed, and therefore friction modeling and compensation is a necessity for precise control of the direct-drive manipulators.

The article is organized as follows: Section 2 gives a brief description of different friction phenomena, summaries of existing friction models, and describes the Tustin's model in detail. Section 3 explains the procedures for determining the parameters of the Tustin's model. Section 4 presents the experimental work performed, and finally Sections 5 and 6 present a discussion, and the conclusions respectively.

2. Friction Model

2.1 Friction Mechanism

Main consideration of this paper is the friction at low and medium velocity ranges. For that reason, only these phenomena that are responsible for the existence of friction at these velocities will be outlined. These phenomena are: Coulumb friction, Viscous friction, Static friction and Dahl effect, Negative damping, Timelag, Dwell time, Asymmetry, and History influence[1] [1], some of which have been shown in Figure 2.

1 Due to the space limitations these phenomena will be explained only briefly. For more information about these phenomena, please see [1,4].

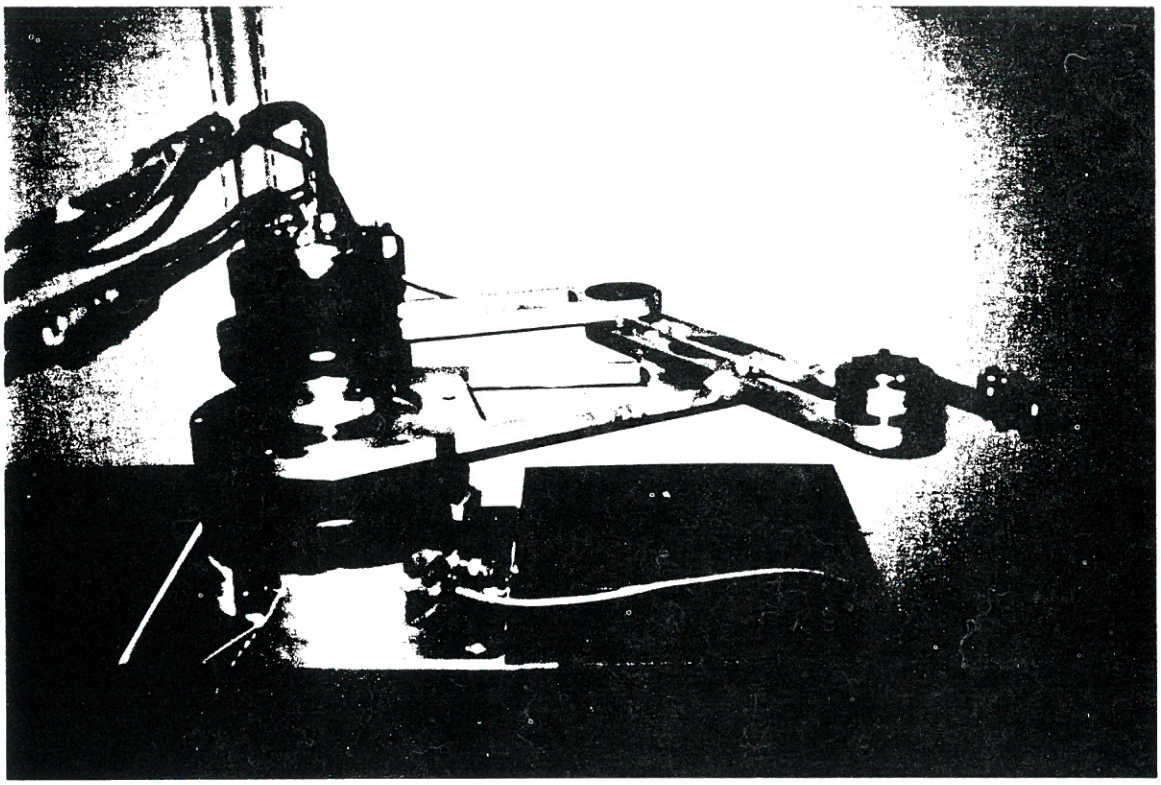

Figure 1. A 2-link Direct-Drive Arm Used for this Study. Motors Are Manufactured by Yokogawa Co. [9]

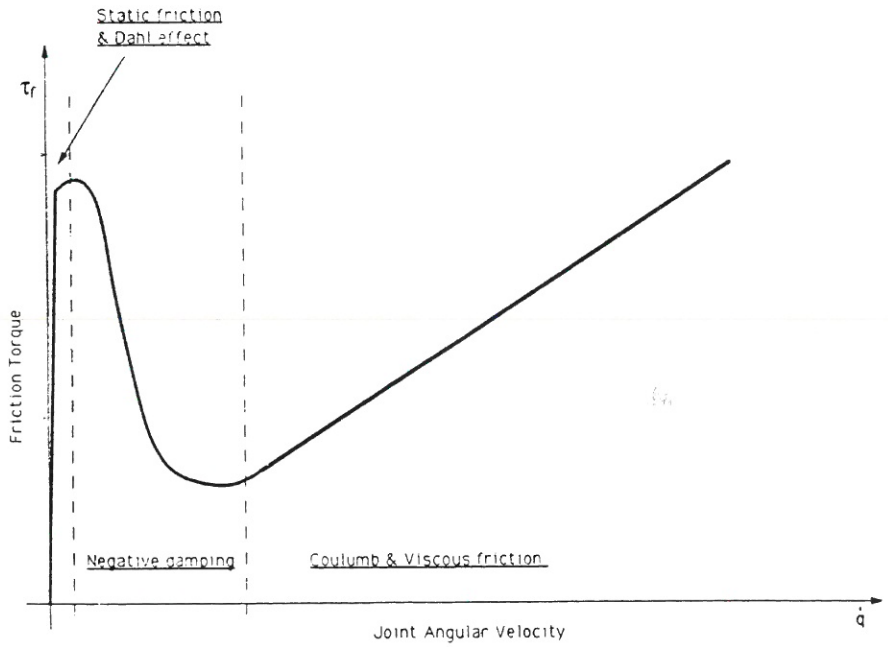

Figure 2. Friction Torque Versus Angular Velocity Characteristics

- **Coulumb friction** is a phenomenon modeled as a constant friction for any velocity, as long as the friction coefficient and "normal" load are unchanged.
- **Viscous friction** is a friction modeled as a linear function of the velocity.
- **Static friction and Dahl effect** are the phenomena that occur just before two sliding surfaces start relative motion. These two effects are usually explained with models of elastic and plastic deformations of the atomic bonds.
- **Negative damping** effect is a result of transition from dry friction (metal-metal friction with no lubricants) towards complete viscous friction. This phenomenon occurs at very low velocities.
- It was found that the Static and the Negative damping frictions increase proportionally with the idle time. This idle time is called the **Dwell time.**
- **Time lag** is the time difference between the moment when certain sliding velocity is reached and the moment when corresponding friction starts act.
- **Asymmetry** is the presence of dissimilar friction models for different sliding directions.
- Finally, it was found that all previous manipulations with sliding surfaces influence the manipulations that follow, and this phenomenon is defined as the **History influence.**

These seven phenomena are considered relevant for low and medium velocity friction compensation. Efficient modeling of these phenomena is crucial for improving the control of the existing robot manipulators.

2.2 Friction Models

Some phenomena mentioned above are very well-known and understood for almost a century, while some others are still extensively studied. However, a number of models have already been proposed and tested in practice. A brief summary of all these models is given in [7]. Even though the summary does not give a detailed description of each model and the method for determining the needed constants, it presents the major advantages, disadvantages, the main parameters, and the phenomena that the models are addressing. From this summary it was found that a majority of models include Coulumb friction, Viscous friction, Static friction, Asymmetry and Negative damping. The reason for this is that these phenomena have been recognized as the essential ones, and their modeling as a necessity. On the other hand, Dahl effect, Time lag, Dwell time and History influence are rarely modeled because modeling of these phenomena dramatically increases the complexity of the model. Also, these phenomena are not yet completely understood, and their modeling imposes a number of assumptions.

2.3 Tustin's Model

From a variety of models presented in [7], Tustin's model (Figure 3) was found to be the most suitable for the purpose of this study. This model gives a good approximation of the friction dynamics, it is simple from mathematical point of view, and the constants needed for it can be easily obtained. Tustin's model is defined by the following function. It models the negative damping effect, Coulumb friction, viscous friction, static friction, and asymmetry, efficiently enough. Though the model does not cover Dahl effect, time lag, dwell time, and history influence, it is assumed that it will be capable of modeling real phenomena with relative accuracy.

$$\tau_f = C_0 + C_1 e^{\frac{-|\dot{q}|}{\alpha}} + C_2 |\dot{q}| \qquad (1)$$

where:

$\dot{q}$ ≡ velocity;

τ_f ≡ joint friction;

C_0, C_1 ≡ constants which define the static friction torque;

C_2 ≡ viscous friction constant;

α ≡ time constant of the exponential decay (negative damping);

The model (1) consists of three terms - the constant bias term C_0, the exponential decay term

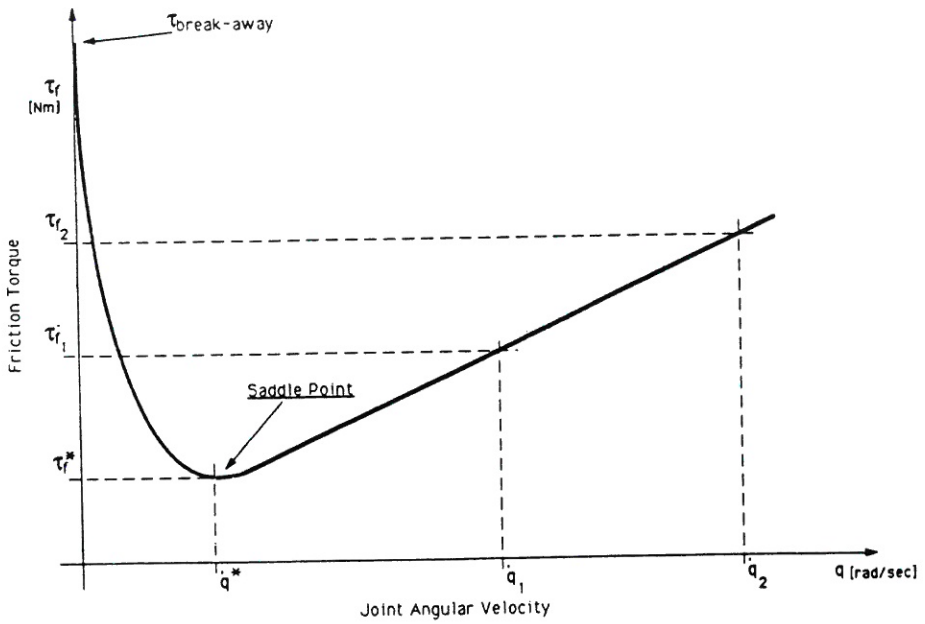

Figure 3. Tustin's Model

$C_1 e^{\frac{-|\dot{q}|}{\alpha}}$, and the linear term $C_2|\dot{q}|$. Static (break-away) friction is modeled with the sum of C_0 and C_1. Negative damping is modeled with exponential decay term $C_1 e^{\frac{-|\dot{q}|}{\alpha}}$, while viscous friction is modeled with the linear term $C_2|\dot{q}|$. Finally, Coulumb friction is modeled with the constant C_0 and asymmetry is obtained by using different constants C_0, C_1, C_2, and α for different sliding directions. In order for the exponential decay component to provide the downward bend in Figure 3, the following condition must be obeyed:

$$\frac{C_2\alpha}{C_1} < 1 \tag{2}$$

The minimum saddle point in the bend is defined by:

$$\dot{q}^* = -\alpha \ln\left(\frac{C_2\alpha}{C_1}\right) \tag{3}$$

then

$$\tau_f(\dot{q}^*) = C_0 + C_2\alpha + C_2\alpha \ln\left(\frac{C_1}{C_2\alpha}\right) \tag{4}$$

For joint speed higher than the value specified by (3), the linear viscous friction (the term $C_2|\dot{q}|$ in (1)) becomes the only significant component of the friction, besides the constant Coulumb friction (modeled as C_0).

3. Parameter Estimation Procedure for Tustin's Model

Obtaining Tustin's friction model requires four parameters to be determined - C_0, C_1, C_2, and α. A procedure to experimentally determine these constants, for each joint of a robot manipulator, is presented in this section. This procedure is based on the assumption that the torque generated at each motor is equal to the command torque. Further, the joint torque is assumed to consist of 3 components as follows:

$$\tau_{appl} = \tau_{inert} + \tau_{fric} = \tau_{tipforce} \quad (5)$$

When the arm is in free motion, $\tau_{tipforce} = 0$. When the arm is in contact with a complaint environment, the tip force F_{tip} is measured using a force sensor and the corresponding joint torque $\tau_{tipforce}$ is calculated from the arm Jacobian **J** as:

$$\tau_{tipforce} = \mathbf{J}^T F_{tip} \quad (6)$$

During the experiments performed, the velocity was constant ($\tau_{inert} = 0$), and the robot arm was in free motion ($\tau_{tipforce} = 0$), so that $\tau_{appl} = \tau_{fric}$.

3.1 Parameters C_0 and C_2

For this, we consider reltively large velocities, $|\dot{q}| >>> 0$, at which Tustin's model in (1) reduces to:

$$\tau_f = C_0 + C_2|\dot{q}| \quad (7)$$

This is quite obvious from the linear portion of the Tustin's curve shown in Figure 3, that describes τ_f for $\dot{q} > \dot{q}^*$. This portion is in fact described by Equation 7. The slope of that line can be calculated as:

$$C_2 = \frac{\tau_{f1} - \tau_{f2}}{|\dot{q}_1| - |\dot{q}_2|} \quad (8)$$

where τ_{f1} and τ_{f2} are two friction torques corresponding to two velocities $\dot{q}_1$ and $\dot{q}_2$, respectively.

Procedure:

Step 1. Move the joint with a relatively large velocity $\dot{q}_1$.

Step 2. Obtain the constant input torque (=generated torque), τ_{f1}.

Step 3. Repeat steps 1 and 2 for a different velocity $\dot{q}_2$.

Step 4. Calculate C_2 from (8), and then C_0 from (7), respectively.

3.2 Parameter C_1

At, $|\dot{q}| = 0$, Equation 1. reduces to:

$$\tau_f = C_0 + C_1 = \tau_{break\text{-}away} \quad (9)$$

Procedure:

Step 1. Initially, let the joint be stationary ($\dot{q} = 0$). Gradually increase joint torque in very small steps.

Step 2. Watch out for the instant at which the joint starts moving. The corresponding friction torque is the $\tau_{break\text{-}away}$.

Step 3. Calculate C_1 from (9), since C_0 is already known.

3.3 Parameter α

The joint velocity $\dot{q}^*$ corresponding to the saddle point of the Tustin's curve in Figure 3 was obtained earlier in (3). Since we already know C_1 and C_2, we can calculate α from (3). Notably, this relation is a non-linear function of α and can yield an infinite number of solutions. This problem can be overcome as follows. Let us first re-write the above expression as:

$$C_1 e^{\frac{-\dot{q}}{\alpha}} = C_2 \alpha \quad (10)$$

Now, consider Tustin's model (1). By rearranging terms and considering the saddle point only, we can re-write it as:

$$C_1 e^{\frac{-|\dot{q}^*|}{\alpha}} = \tau_f^* - C_0 - C_2|\dot{q}^*| \quad (11)$$

We then equate the RHS of (10) with (11), and rearrange the terms to get:

$$\alpha = \frac{1}{C_2}\left(\tau_f^* - C_0 - C_2|\dot{q}^*|\right) \quad (12)$$

Now, we can obtain τ_f^* and $\dot{q}^*$ experimentally, then calculate α from this expression.

Procedure:

Step 1. Obtain a plot of τ_f and $\dot{q}$ at relatively low velocities.

Step 2. From the data, determine τ_f^* and $\dot{q}^*$ corresponding to the saddle point.

Step 3. Calculate α from (12)

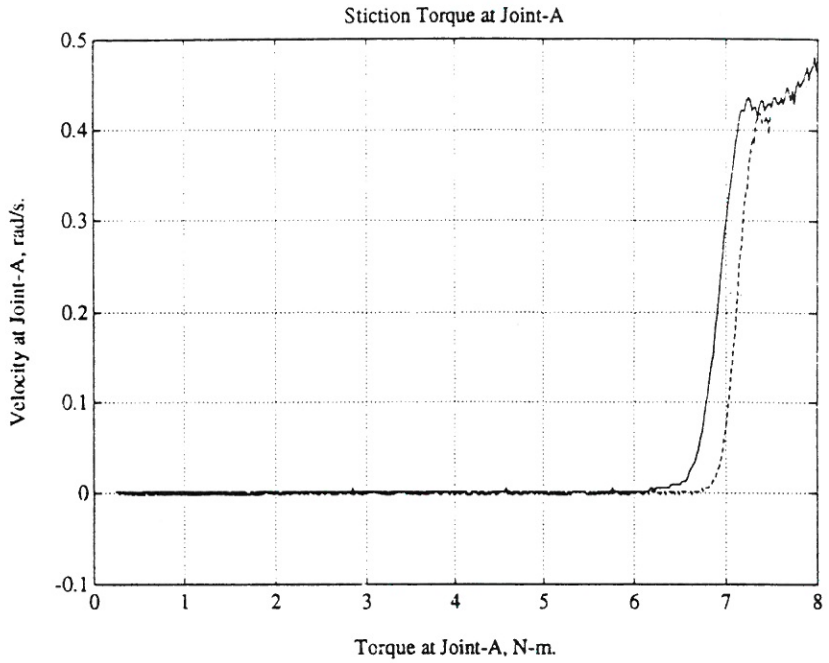

Figure 4.Joint A's Torques Versus Angular Velocity Characteristics from Break-away Experiment

4. Experiments

The experimental arm is a 2-link planar-bar mechanism (Figure 1), actuated by two brushless, permanent magnet DC (direct-drive) motors - DMA 1050 and DMB 1035, manufactured by Yokogawa Co. [9]. The arm is controlled via a Compaq 386/25 PC.

The control programs were written in C language. The control frequency in all experiments reported here was 80 Hz (12.5 mses sample time). Two sets of experiments were performed:

- Break-away torque determination;
- Torque-velocity relationship determination;

Details of these experiments are presented below.

4.1 Break-away (Friction) Torque

Break -away torque is the minimum torque necessary to move a joint from rest. Such torque is denoted by $\tau_{break\text{-}away}$ in Figure 3, and it was determined in our experiment as follows.

First, only Joint A was considered for the test, while Joint B was held stationary at a suitable position, using a PID scheme. A gradually increasing torque was applied to Joint A in open-loop. The torque increment per sample period was 0.02 Nm. At each instant, the joint velocity and applied torque were recorded. When the applied torque reached a value equal to the break-away torque, Joint A started to move, as indicated by the joint velocity value. The joint velocity and torque of Joint A were recorded over the entire event. Corresponding velocity plots for four trials are given in Figure 4. The experiment was repeated several times to examine the repeatability. Break-away torque $\tau_{A\,break\text{-}away}$ was taken to be the average of 10 readings. Clearly,

$\tau_{A\ break\text{-}away} \simeq 6.25$ Nm from Figure 4. Similar trials were performed on Joint B while holding Joint A stationary in a suitable position using PID control. With an increment in torque of 0.005 Nm/sample, the obtained break-away torque was,

$\tau_{B break\text{-}away} \simeq 2.8$ Nm.

4.2 Torque-Velocity Relationship

First, Joint B was held stationary via a PID position regulation scheme. Joint A was commanded to move with a desired constant velocity, also using the PID control scheme.

During each experiment, the desired constant velocity was specified while the actual velocity and applied torque were recorded over the event. As an example, the results at a very small velocity (0.03 rad/sec) are given in Figure 5. It is shown that moving Joint A with a velocity of 0.03 rad/sec (Figure 5.a) requires overcoming an average friction torque of 6.5 Nm (Figure 5.b). The experiment was repeated for different velocities over the range 0.0075 to 1.0 rad/sec. For each value, 4 trials were performed and their average was calculated. The torque-velocity data obtained, along with the $\tau_{A\ break\text{-}away}$ value obtained earlier, were fitted with a curve as shown in Figure 6. Note that the chosen friction model (1) is a non-linear function of the velocity parameterized by constants C_0, C_1, C_2, and α. This does not allow curve fitting via least-squares method and hence, we resorted to fitting the curve by a trial and error method. Furthermore, the clear-cut procedure detailed in Section 3 could not be used because the experimental data were highly scattered, particularly at low velocity ranges. The same procedure was repeated for Joint B with Joint A held stationary and the corresponding torque velocity relationship as shown in Figure 7.

4.3 Model-based Compensation

The precision of the models determined above was further verified by using them in a model-based feedforward compensation. The nominal controller was a PD:

$$\tau = K_p q_e + K_v \dot{q}_e \qquad (13)$$

and when compensation was applied became:

$$\tau = K_p q_e + K_v \dot{q}_e + \tau_f \qquad (14)$$

where τ_f was the model-based torque to overcome friction.

Logically, the position error is expected to be smaller when compensation is applied. The difference in the position errors with and without compensation should have a pronounced effect at lower than at larger velocities. Furthermore, if the PD gains are relatively large, the effect of friction compensation will not be distinct. In summary, the effectiveness of compensation depends upon two factors: the velocity and the gains. Here, we have studied the effectiveness of compensation at two different velocities and two different sets of gains. In particular, the velocities used were 0.5 rad/sec and 0.05 rad/sec, while the position gains chosen were 60 and 30, from which the velocity gains were calculated as $K_v = 2\sqrt{K_p}$ for critical damping under the assumption that the system was operating in the linear region.

4.3.1 Compensation at High Velocities

As stated above, the extent of model-based compensation varies with the control gains used in the nominal PD controller. At the chosen velocity of 0.5 rad/sec, two tests were performed with $K_p = 60$ and 30 respectively. The resulting position errors in the two tests are shown in Figure 8. As noticed, the position error with compensation (solid line) is better than that with no compensation (dotted line) in both cases of high and low values of K_p. Moreover, the compensated position error for $K_p = 60$ is smaller than that for $K_p = 30$. This indicates that the larger gains offset the effect of friction to some extent, therefore the model based compensation is less effective when using larger gains in the associated controller.

4.3.2 Compensation at Low Velocities

For the same position and velocity gains as before ($K_p = 60$ and 30), but for a lower velocity of 0.05 rad/sec, the experiments were repeated with and without compensation and the results are shown in Figure 9. As seen, the position error with friction compensation is smaller than without

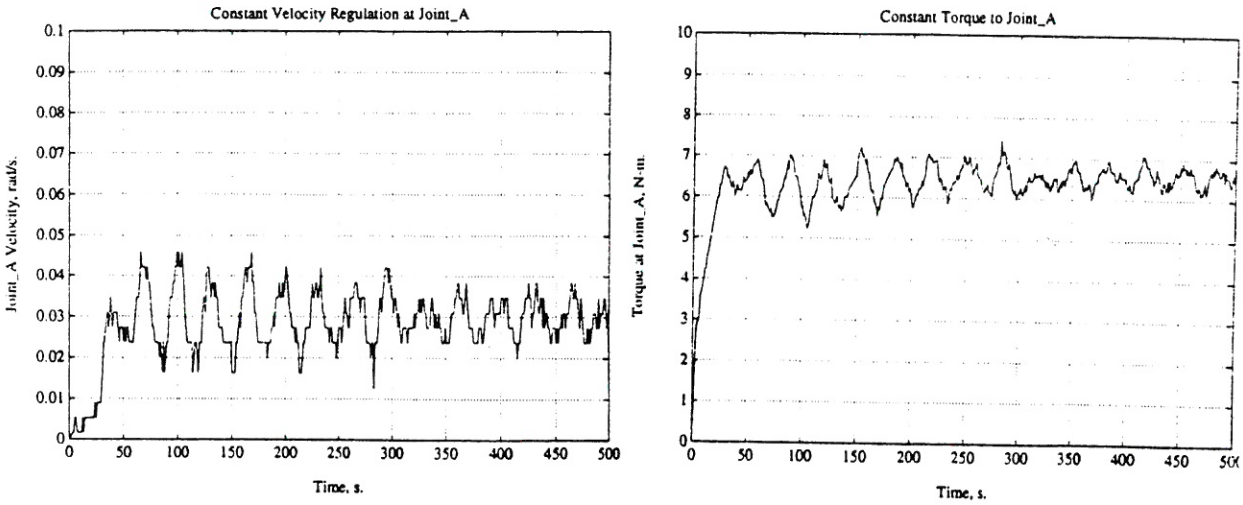

Figure 5. Torque and Angular Velocity Characteristics of the Joint A

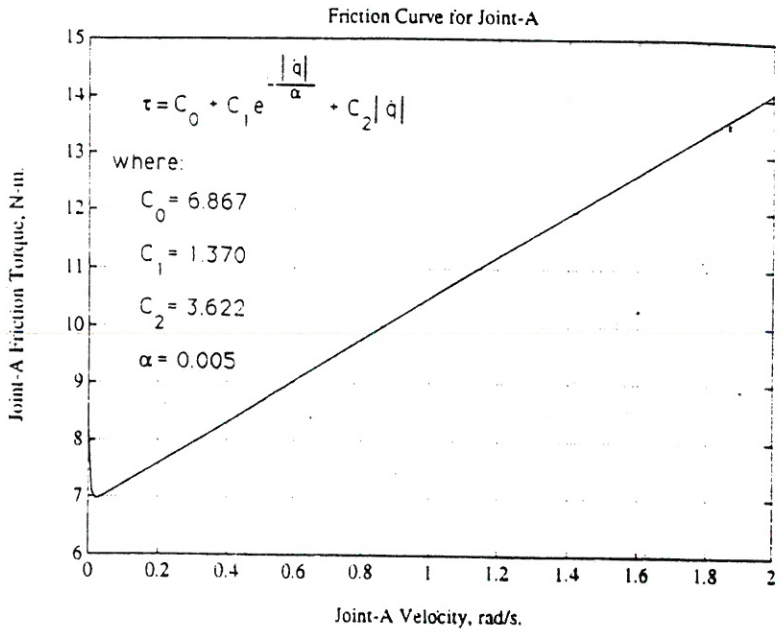

Figure 6. Tustin's Model form the Joint A

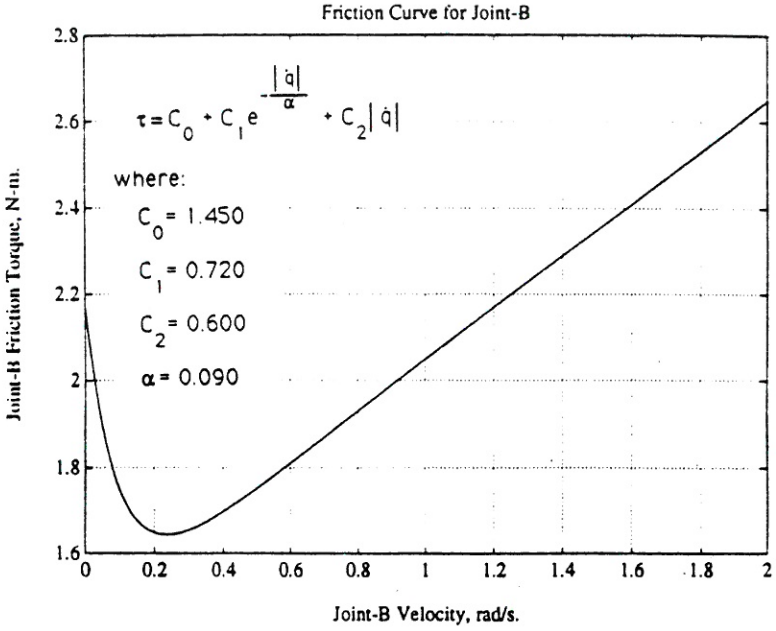

Figure 7. Tustin's Model for the Joint B

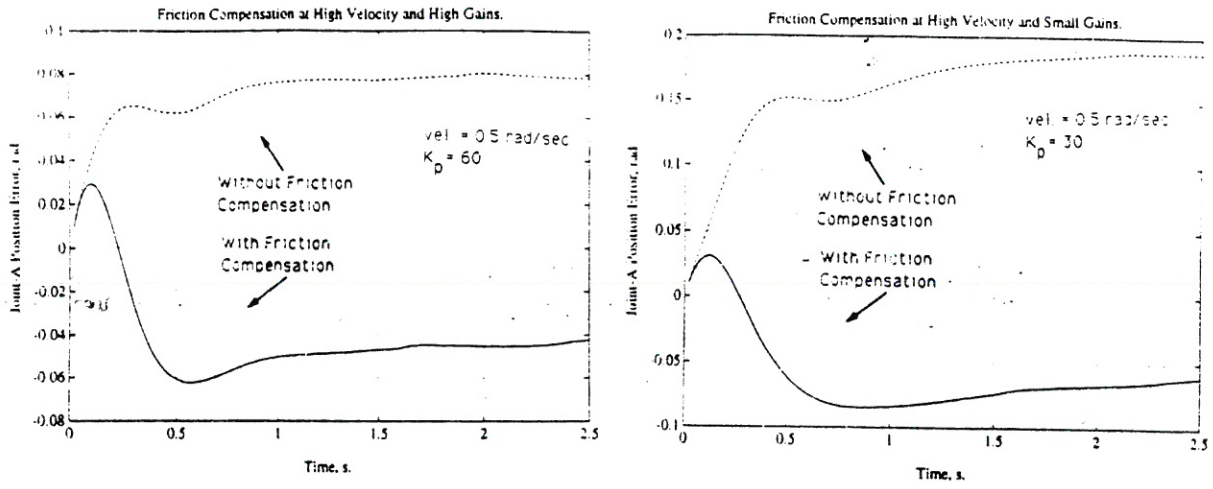

Figure 8. Joint Error with and without Friction Compensation for Joint A at High Velocity with High and Low Gains

compensation. Again, the position errors were smaller at larger gains. This was further confirmed by repeating the experiments on Joint B (Figure 10).

From Figures 9 and 10 we conclude that the control gain offsets the effect of friction to some extent and hence it is difficult to see the extent of compensation. However, with a smaller gain, the compensation is seen to have a more pronounced effect. That is, the extent of compensation is higher when the control gains as well as the desired velocity are low. Also to note are the initial oscillations in Figure 10, both for low and high gains. They are possibly the limit cycles resulting from the stick-slip process.

5. Discussion

In summary, the results verify that the parameters of the Tustin model determined experimentally are reasonably precise. As the parameters could not be determined exactly, we could not achieve zero position errors in all trials when compensation was applied. This implies that the extent of compensation largely depends on the precision of the estimated model. For a given robot and its associated hardware, the friction model can be obtained with an utmost precision of about 90% [1]. This further depends on the nature of the trajectory chosen for estimation and the signal to noise ratio of the joint sensors [3]. Additionally, as found in our work, the precision of the estimated model also depends on the prior history of the joint in question.

The point to note above is that it is impossible to practically obtain a precise friction model in any given system. Therefore, a model-based compensation always results in either an under-compensation or an over-compensation. Under-compensation results when the estimated friction is smaller in magnitude than the actual, while an overcompensation occurs when the estimated friction is of larger magnitude than the actual friction. It is easy to show analytically [3] that an overcompensation can cause limit cycles behaviour while an undercompensation can only cause a steady state error.

Possible solutions to avoid over - and under-compensation are the use of adaptive [2, 3] and robust [8] control schemes in association with feedforward compensation. Southward et al [8] showed simulation results where the limit cycle behaviour was eliminated while Caundas de Wit et al [2,3] presented an analytical proof of limit cycle avoidance at the stiction point and achieved zero steady state position errors. They demonstrated the results experimentally on a commercial robot arm ACMA-S58.

Both these works do not take into account the same practical aspects of controlling robot arms. Caundas de Wit et al [2, 3] used a square wave trajectory that helped achieve on-line estimation of the friction model in the adaptive control scheme, while a practical trajectory might not be so. Further, the works listed above do not consider the limitations of the hardware - the actuator dynamics, the joint flexibility, the bandwidth of the motor controller, the communication delay, the signal (noise ratio of the joint encoders) pontentiometers and so on. These hardware related issues place constraints on the achievability limit of the gain values in any control scheme. In a situation, when the demanded gains are unachievable, the performance of the control sheme, though it be adaptive or robust, will likely be not much superior to that of simple control scheme such as the PID or a computed torque. This implicitly suggests that it is the dynamics of the robot hardware that ultimately influences the precision with which the friction compensation can be achieved regardless of the basic control scheme or the precision of the estimated model. This argument is further supported by the experimental work separately performed in our laboratory [6] wherein several robust schemes were experimentally compared for their performance evaluation.

6. Conclusion

This paper presented the results of our experiments with a two link direct-drive manipulator whose friction model was determined and used in model-based feedforward compensation. These results show that the

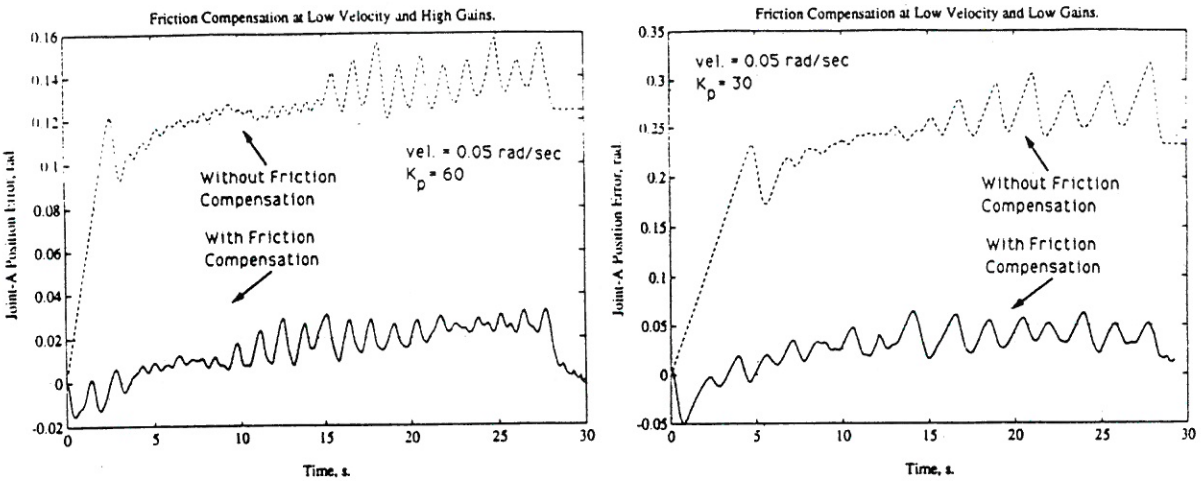

Figure 9. Friction Compensation for Joint A at Low Velocity with High and Low Gains

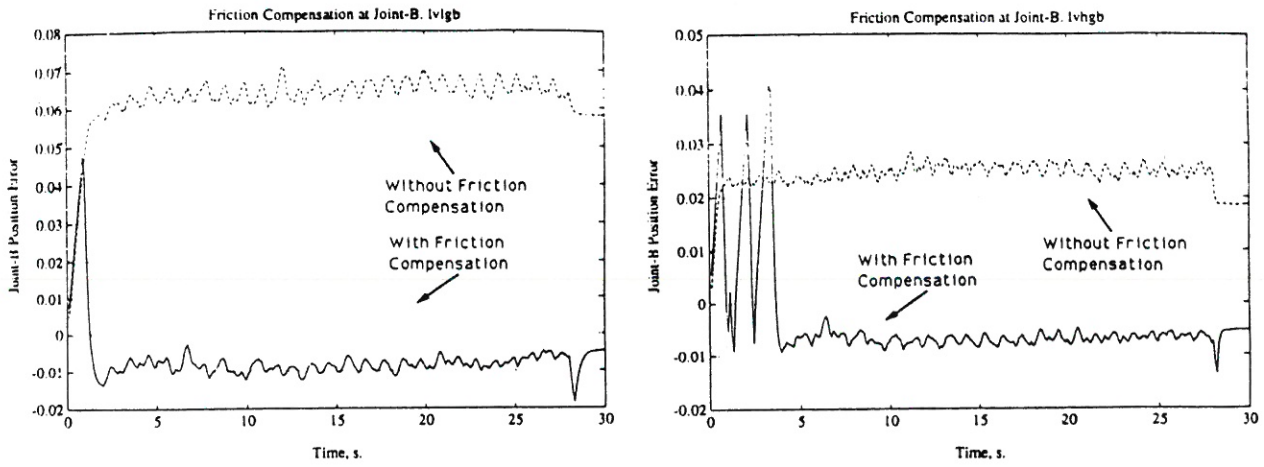

Figure 10. Friction Compensation for Joint B at Low Velocity with High and Low Gains

direct-drive manipulators are not immune from the effects of friction.

Consequently, friction modeling and compensation are important and are necessary for precise control of direct-drive manipulators. The extent of compensation is affected by two factors: the magnitude of velocity and the gains of the basic controller. Better compensation was achieved at smaller velocity and larger gains.

Pointed out is that the computed feedforward compensation, used in the present work, cannot achieve exact compensation. The suggested solution in the literature, the use of adaptive and robust schemes, can also be limited by the hardware if its characteristics are unknown. The precise determination of these characteristics is a very challenging task.

REFERENCES

1. ARMSTRONG, B., **Control of Machines with Friction**, KLUWER ACADEMIC PUBLISHERS, Boston, USA, 1992.
2. CANUDAS DE WIT, C., **Experimental Results on Adaptive Friction Compensation in Robot Manipulators: Low Velocities**, Proceedings of the 1 st International Conference on Experimental Robotics, Montreal, Canada, June 1989, pp. 197-214.
3. CANUDAS DE WIT, C., NOEL, P., AUBIN, A. and BROGLIATO, B., **Adaptive Friction Compensation in Robot Manipulators: Low Velocities**, INTERNATIONAL JOURNAL OF ROBOTICS RESEARCH, Vol.1,1991.
4. DAHL, P.R., **Measurement of Solid Friction Parameters of Ball Bearings**, Proc. of 6th Annual Symp. on Incremental Motion, Control System Devices, University of Illinois, 1977.
5. LING, F.F., KLAUS, E.E. and FEIN, R.S., **Boundary Lubrication - An Appraisal of World Literature**, The American Society of Mechanical Engineers, New York, USA, 1965.
6. LIU, G.J. and GOLDENBERG, A.A., 1992, **Experiments on Robust Control of Robot Manipulators**, Proceedings of 1992 IEEE International Conference on Robotics and Automation, Nice, France, May 10-12, 1992.
7. POPOVIC, M.R., SHIMOGA, K.B., HUI, R.C., and GOLDENBERG, A.A., **Modeling and Compensation of Friction in Direct-Drive Robotic Arms**, International Conference on CAD/CAM Robotics and Factories of the Future, St. Petersburg, Russia, May 1993.
8. SOUTHWARD, S.C., RADCLIFF, C.L. and MACCLUER, C.R., **Robust Nonlinear Stick-slip Friction Compensation**, Presented at the ASME Winter Annual Meeting, Dallas, TX, November 1990, Paper No. 90-WA/DSC-8, 7 pages.
9. YOKOGAWA, **Product Literature on DMA and DMB Series Direct-drive Motors**, Yokogawa Corporation of America, Lake Geneva, MI., 1989.